SCIENCE CHINA
Information Sciences

• RESEARCH PAPER •

May 2022, Vol. 65 152301:1–152301:15
https://doi.org/10.1007/s11432-021-3313-9

# Joint optimization of spectral efficiency and energy efficiency with low-precision ADCs in cell-free massive MIMO systems

Han WANG[1], Chang SUN[1], Jiamin LI[1,2*], Pengcheng ZHU[1], Dongming WANG[1,2] & Xiaohu YOU[1,2]

[1]*National Mobile Communications Research Laboratory, Southeast University, Nanjing* 210096, *China;*
[2]*Purple Mountain Laboratories, Nanjing* 211111, *China*

Received 4 May 2021/Revised 9 July 2021/Accepted 9 August 2021/Published online 23 March 2022

**Abstract** In cell-free massive multiple-input multiple-output (MIMO) systems, it is beneficial to apply low-precision analog-to-digital converters (ADCs) to reduce power consumption, hardware cost, and the load on backhaul link. However, low-precision ADCs will result in serious degradation in spectral efficiency (SE). It is important to achieve a good tradeoff between SE and energy efficiency (EE) for cell-free massive MIMO systems with low-precision ADCs. In this paper, we first derive the closed-form expressions of uplink achievable rates with maximal ratio combining (MRC) receiver and zero-forcing (ZF) receiver in cell-free massive MIMO systems. Then we analyze the EE model of cell-free massive MIMO systems. Based on the above analysis, the tradeoff between SE and EE is studied. Moreover, we propose two quantization bit allocation algorithms to optimize the SE and EE jointly from the perspective of multi-objective optimization. One algorithm is based on the deep Q-network (DQN) and the other one is based on the non-dominated sorting genetic algorithm II (NSGA-II). The proposed algorithms provide more feasible solutions and achieve better system performance than equal quantization bit allocation algorithm. Numerical results verify the accuracy of the derived closed-form expressions and the effectiveness of the proposed optimization algorithms.

**Keywords** cell-free massive MIMO, low-precision ADC, spectral efficiency, energy efficiency, multi-objective optimization

**Citation** Wang H, Sun C, Li J M, et al. Joint optimization of spectral efficiency and energy efficiency with low-precision ADCs in cell-free massive MIMO systems. Sci China Inf Sci, 2022, 65(5): 152301, https://doi.org/10.1007/s11432-021-3313-9

## 1 Introduction

In cell-free massive multiple-input multiple-output (MIMO) systems, a large number of remote antenna units (RAUs) are connected to a central processing unit (CPU) and distributed over a large area to coherently serve a small number of users. Benefiting from the above merits, cell-free massive MIMO systems have the potential to enhance the system performance greatly in the beyond fifth-generation (B5G) and the sixth-generation (6G) networks [1].

However, the hardware complexity, power consumption of analog-to-digital converters (ADCs) in radio frequency (RF) chains and capacity requirement on the link between CPU and RAUs increase exponentially with the number of quantization bit. Therefore, one of the possible ways to reduce cost is using low-precision ADCs which has received widespread attention in recent years.

Considerable research studies have been conducted to study the influence of low-precision ADCs on spectral efficiency (SE) and energy efficiency (EE). But the tradeoff between SE and EE is not mentioned in detail. Refs. [2–5] studied the impact of low-precision ADCs on SE. On the condition that the precision of ADCs on the same RAUs was the same, the downlink and uplink achievable rates of distributed massive MIMO systems with low-precision ADCs were analyzed respectively in [2, 3]. However, all RAUs were

* Corresponding author (email: jiaminli@seu.edu.cn)

 

assumed to transmit and receive signals independently. Ref. [4] found 6-bit precision ADCs can achieve the same performance as the perfect ADCs. Ref. [5] showed the impacts of the key design parameters that include the number of total antenna arrays and the proportion of ideal ADCs/digital-to-analog converters (DACs) on the uplink achievable rates in cell-free massive MIMO systems with mixed-ADC/DAC receiver. Refs. [6,7] studied the impact of low-precision ADCs on EE. Ref. [6] pointed out low-precision ADCs were not recommended from an EE point of view. Ref. [7] compared the EE with zero-forcing (ZF) receiver and with ZF successive interference cancellation (ZF-SIC) receiver in uplink cell-free massive MIMO systems with low-precision ADCs.

Besides, the optimization of SE and EE in cell-free massive MIMO systems with low-precision ADCs has been discussed in [8–11]. Ref. [8] formulated an optimization problem to determine the portion of the antennas connected to the low-power one-bit ADCs at the base station (BS) to maximize the sum SE for a given budget constraint in single-cell multiuser MIMO systems. Ref. [9] proposed a quantized bit allocation mechanism based on sum rate maximization and the superiority of the mechanism was proved. EE can be maximized by optimizing the number of quantization bit and antenna selection in MIMO systems [10]. But above researches only consider SE maximization or EE maximization separately. EE decreases monotonically with the increase of SE, so the EE and SE cannot be maximized simultaneously in terms of the quantization bit allocation. An ADC resolution optimization algorithm was proposed in [11] to maximize a linear combination of SE and power consumption of BS. But the solutions obtained by the algorithm only achieved the same performance as the equal quantization bit allocation algorithm. The equal quantization bit allocation is easy to implement but cannot maximize the SE and EE.

Motivated by the above observations, this paper analyzes the impact of low-precision ADCs on the SE and EE performance of cell-free massive MIMO systems, and proposes two quantization bit allocation algorithms to maximize SE and EE jointly from the perspective of multi-objective optimization. The main contributions of this paper are summarized as follows.

- Considering maximal ratio combining (MRC) receiver and ZF receiver, we derive the closed-form expressions of the uplink achievable rates based on the estimated channel state information (CSI) at RAUs and additive quantization noise model (AQNM). Besides, we build the power consumption model and EE model in cell-free massive MIMO systems.
- Based on the closed-form expressions of SE and EE, we take insight into the tradeoff between SE and EE in terms of the number of antennas per RAU, the transmit power per user and the number of quantization bit.
- To jointly optimize SE and EE, we propose two quantization bit allocation algorithms subject to the total ADC quantization bit constraint and quality-of-service (QoS) constraint. The proposed bit allocation algorithms achieve better performance and provide more feasible solutions to the allocation of quantization bit. The simulation results show the proposed algorithms outperform the equal quantization bit allocation algorithm.

The rest of this paper is organized as follows. System models consisting of cell-free massive MIMO systems channel model, quantization noise model and uplink channel estimation are discussed in Section 2. Then in Section 3, we derive the closed-form expressions of the uplink achievable rates and model the system power consumption and EE. Besides, we propose two quantization bit allocation algorithms based on the deep Q-network (DQN) and the non-dominated sorting genetic algorithm II (NSGA-II) in Section 4, respectively. Simulation results and discussions are presented in Section 5. Lastly, in Section 6, we summarize our contributions and draw conclusions.

Notation. Vectors and matrices are denoted by boldface lower case and upper case letters, respectively. $\mathbf{I}_N$ denotes an $N$-dimensional identity matrix. $(\cdot)^{\mathrm{T}}$ and $(\cdot)^{\mathrm{H}}$ represent the transpose operator and conjugate transpose operator, respectively. $|\cdot|$ and $\|\cdot\|$ represent the absolute value of a scalar and spectral norm of a matrix, respectively. $\mathbb{E}[\cdot]$, $\mathbb{E}[\cdot|\cdot]$ and $\mathrm{Cov}(\cdot,\cdot)$ denote the expectation, conditional expectation and covariance operator, respectively. $\mathrm{diag}\{\cdot\}$ denotes a square diagonal matrix with the elements of the given vector on the main diagonal. $\otimes$ is the Kronecker product. $\boldsymbol{h} \sim \mathcal{CN}(0, \mathbf{I}_N)$ denotes vector $\boldsymbol{h}$ satisfies circularly symmetric complex Gaussian distribution with mean zero and covariance matrix $\mathbf{I}_N$.

## 2 System model

We consider an uplink cell-free massive MIMO system with $K$ users served by $M$ RAUs. Each RAU is equipped with $N$ antennas and the RF chain of each antenna includes an ADC. The precision of ADCs

at one RAU is the same and that is irrelevant at different RAUs. All RAUs are connected via backhaul links to the CPU where the design of receivers and the processing of received signals are completed. All RAUs cooperate to receive signals but each RAU quantizes signals separately.

### 2.1 Channel model

The uplink channel vector between all RAUs and the $k$-th users is assumed to be frequency-flat fading and is modeled as

$$\boldsymbol{g}_k = \left[\sqrt{\lambda_{1,k}}\boldsymbol{h}_{1,k}^{\mathrm{T}}, \sqrt{\lambda_{2,k}}\boldsymbol{h}_{2,k}^{\mathrm{T}}, \ldots, \sqrt{\lambda_{M,k}}\boldsymbol{h}_{M,k}^{\mathrm{T}}\right]^{\mathrm{T}}, \tag{1}$$

where $\lambda_{m,k}$ represents the pass lose between the $m$-th RAU and the $k$-th user which depends on the distance between them, $\boldsymbol{h}_{m,k} \sim \mathcal{CN}(0, \mathbf{I}_N) \in \mathbb{C}^{N\times 1}$ represents small-scale fast fading. Thus, $\mathbb{E}\left[\boldsymbol{g}_k \boldsymbol{g}_k^{\mathrm{H}}\right] = \boldsymbol{\Lambda}_k = \mathrm{diag}\left(\lambda_{1,k}, \lambda_{2,k}, \ldots, \lambda_{M,k}\right) \otimes \mathbf{I}_N$, and $\boldsymbol{g}_k \sim \mathcal{CN}(0, \boldsymbol{\Lambda}_k)$.

### 2.2 Quantization noise model

In uplink transmission, the signal of $K$ users received by the $m$-th RAU can be written as

$$\boldsymbol{y}_m = \sqrt{p_{\mathrm{u}}} \sum_{k=1}^{K} \boldsymbol{g}_{m,k} x_k + \boldsymbol{n}_m, \tag{2}$$

where $x_k$ denotes the Gaussian-distributed signal with zero mean from the $k$-th user, $\boldsymbol{g}_{m,k}$ denotes the channel vector between the $m$-th RAU and the $k$-th user, $\sqrt{p_{\mathrm{u}}}$ denotes uplink transmitted power per user, $\boldsymbol{n}_m \sim \mathcal{CN}\left(0, \sigma^2 \mathbf{I}_N\right) \in \mathbb{C}^{N\times 1}$ is the complex additive white Gaussian noise (AWGN) vector whose elements are mutually independent and have zero means [2, 7], and $\sigma^2$ is the power of noise.

Then, the quantized signal is expressed as

$$\boldsymbol{y}_{m\mathrm{q}} = Q\left(\boldsymbol{y}_m\right) = Q\left(\sqrt{p_{\mathrm{u}}} \sum_{k=1}^{K} \boldsymbol{g}_{m,k} x_k + \boldsymbol{n}_m\right), \tag{3}$$

where $Q(\cdot)$ represents quantization function. Quantization noise can be modeled as AQNM when the gain is set appropriately by automatic gain control (AGC). Hence, quantized received signal is given by

$$\boldsymbol{y}_{m\mathrm{q}} \approx \alpha_m \boldsymbol{y}_m + \boldsymbol{n}_{m\mathrm{q}} = \sqrt{p_{\mathrm{u}}}\alpha_m \sum_{k=1}^{K} \boldsymbol{g}_{m,k} x_k + \alpha_m \boldsymbol{n}_m + \boldsymbol{n}_{m\mathrm{q}}, \tag{4}$$

where $\alpha_m = 1 - \rho_m$, $\rho_m$ represents the reciprocal of signal to quantization noise ratio at the $m$-th RAU and depends on the number of quantization bit. It is assumed that the input of the quantizer satisfies Gaussian distribution and $b$ represents the number of quantization bit. For a Gaussian random variable non-uniform scalar least mean square error quantizer, the value of $\rho$ is given in Table 1 when $b \leqslant 5$ . When $b > 5$, $\rho$ can be approximated as $\rho = \frac{\pi\sqrt{3}}{2} \cdot 2^{-2b}$. $\boldsymbol{n}_{m\mathrm{q}}$ denotes the additive quantization noise vector whose elements satisfy the complex Gaussian distribution with zero mean and are mutually independent [2, 7]. According to [5], the covariance of $\boldsymbol{n}_{m\mathrm{q}}$ for fixed channel is

$$\boldsymbol{R}_{\boldsymbol{n}_{m\mathrm{q}}, \boldsymbol{n}_{m\mathrm{q}}} = \alpha_m \left(1 - \alpha_m\right) \mathrm{diag}\left(\mathbb{E}\left[\boldsymbol{y}_m \boldsymbol{y}_m^{\mathrm{H}}\right]\right). \tag{5}$$

Therefore, the signal received by all RAUs is written as

$$\boldsymbol{y} = \sqrt{p_{\mathrm{u}}}\boldsymbol{G}\boldsymbol{x} + \boldsymbol{n}, \tag{6}$$

where $\boldsymbol{x} \in \mathbb{C}^{K\times 1}$ denotes the data signal from $K$ users, $\sqrt{p_{\mathrm{u}}}$ denotes uplink transmitted power per user, $\boldsymbol{n} = [\boldsymbol{n}_1^{\mathrm{T}}, \boldsymbol{n}_2^{\mathrm{T}}, \ldots, \boldsymbol{n}_M^{\mathrm{T}}]^{\mathrm{T}} \sim \mathcal{CN}\left(0, \sigma^2 \mathbf{I}_{MN}\right) \in \mathbb{C}^{MN\times 1}$ is the complex AWGN, $\sigma^2$ is the power of noise, $\boldsymbol{G} = [\boldsymbol{g}_1, \boldsymbol{g}_2, \ldots, \boldsymbol{g}_K] \in \mathbb{C}^{MN\times K}$ represents the channel matrix between all the $M$ RAUs and all the $K$ users, $\boldsymbol{g}_k = [\boldsymbol{g}_{1,k}^{\mathrm{T}}, \boldsymbol{g}_{2,k}^{\mathrm{T}}, \ldots, \boldsymbol{g}_{M,k}^{\mathrm{T}}]^{\mathrm{T}} \in \mathbb{C}^{MN\times 1}$ represents the channel vector between $M$ RAUs and the $k$-th user.

Under the AQNM, the quantized received signal of all RAUs is written as

$$\boldsymbol{y}_{\mathrm{q}} \approx \boldsymbol{A}\boldsymbol{y} + \boldsymbol{n}_{\mathrm{q}} = \sqrt{p_{\mathrm{u}}}\boldsymbol{A}\boldsymbol{G}\boldsymbol{x} + \boldsymbol{A}\boldsymbol{n} + \boldsymbol{n}_{\mathrm{q}}, \tag{7}$$

**Table 1** The values of $\rho$ for different $b$

| | $b=1$ | $b=2$ | $b=3$ | $b=4$ | $b=5$ |
|---|---|---|---|---|---|
| $\rho$ | 0.3634 | 0.1175 | 0.03454 | 0.009497 | 0.002499 |

where $\boldsymbol{A}=\operatorname{diag}(\alpha_1,\alpha_2,\ldots,\alpha_M)\otimes\mathbf{I}_N$, $\boldsymbol{n}_{\mathrm{q}}=[\boldsymbol{n}_{1\mathrm{q}}^{\mathrm{T}},\boldsymbol{n}_{2\mathrm{q}}^{\mathrm{T}},\ldots\boldsymbol{n}_{M\mathrm{q}}^{\mathrm{T}}]^{\mathrm{T}}$. The signal $\boldsymbol{x}$, the complex AWGN $\boldsymbol{n}$ and the quantization noise $\boldsymbol{n}_{\mathrm{q}}$ are mutually independent [7].

Due to the independence of quantization noise, the covariance of $\boldsymbol{n}_{\mathrm{q}}$ for fixed channel is

$$\begin{aligned}\boldsymbol{R}_{\boldsymbol{n}_{\mathrm{q}},\boldsymbol{n}_{\mathrm{q}}}&=\mathbb{E}\left[\boldsymbol{n}_{\mathrm{q}}{\boldsymbol{n}_{\mathrm{q}}}^{\mathrm{H}}\right]\\&=\mathbb{E}\left[\operatorname{diag}(\boldsymbol{n}_{1\mathrm{q}}\boldsymbol{n}_{1\mathrm{q}}^{\mathrm{H}},\boldsymbol{n}_{2\mathrm{q}}\boldsymbol{n}_{2\mathrm{q}}^{\mathrm{H}},\ldots,\boldsymbol{n}_{M\mathrm{q}}\boldsymbol{n}_{M\mathrm{q}}^{\mathrm{H}})\right]\\&=\boldsymbol{A}\left(\mathbf{I}-\boldsymbol{A}\right)\left(p_{\mathrm{u}}\sum_{j=1}^{K}\boldsymbol{\Lambda}_j+\sigma^2\mathbf{I}\right),\end{aligned}\tag{8}$$

where $\boldsymbol{\Lambda}_j=\mathbb{E}\left[\boldsymbol{g}_j\boldsymbol{g}_j^{\mathrm{H}}\right]=\operatorname{diag}(\lambda_{1,j},\lambda_{2,j},\ldots,\lambda_{M,j})\otimes\mathbf{I}_N$.

### 2.3 Channel estimation with low-precision ADCs

It is assumed that the CSI is unknown at RAUs and channel estimation via pilot training is necessary. The pilot sequences are quantified by low-precision ADCs at RAUs and then sent to the CPU for channel estimation, so the low-precision ADCs will bring an adverse effect on channel estimation. However, it is more practical to take the quantization process into consideration when estimating channels.

During the uplink pilot transmission phase, the orthogonal pilot sequences of all users are represented by $\boldsymbol{X}_{\mathrm{p}}$ and the length of pilot sequences is $K$. To facilitate analysis, $\boldsymbol{X}_{\mathrm{p}}$ is assumed to be $K\times K$ unit matrix $\mathbf{I}_K$ [12,13]. Therefore, the quantized pilot signal received by all RAUs is expressed as

$$\boldsymbol{Y}_{\mathrm{p}}\approx\sqrt{p_{\mathrm{p}}}\boldsymbol{A}\boldsymbol{G}\boldsymbol{X}_{\mathrm{p}}+\boldsymbol{A}\boldsymbol{N}+\boldsymbol{N}_{\mathrm{q}},\tag{9}$$

where $p_{\mathrm{p}}$ is the power of pilot signal, $\boldsymbol{N}\in\mathbb{C}^{MN\times K}$ denotes the AWGN matrix with $\mathcal{CN}\left(0,\sigma^2\right)$ elements, $\boldsymbol{N}_{\mathrm{q}}\in\mathbb{C}^{MN\times K}$ denotes the additive Gaussian quantization noise matrix which is uncorrelated with the unquantized received signal. Then the received pilot signal of the $k$-th user at RAUs is written as

$$\boldsymbol{y}_{k\mathrm{p}}\approx\sqrt{p_{\mathrm{p}}}\boldsymbol{A}\boldsymbol{g}_k+\boldsymbol{A}\boldsymbol{n}_k+\boldsymbol{n}_{k\mathrm{q}},\tag{10}$$

where $\boldsymbol{n}_k$ denotes the $k$-th column of $\boldsymbol{N}$ and $\boldsymbol{n}_{k\mathrm{q}}$ denotes the $k$-th column of $\boldsymbol{N}_{\mathrm{q}}$.

The minimum mean-square error (MMSE) channel estimation of the uplink channel from the $k$-th user to all the RAUs is given by

$$\hat{\boldsymbol{g}}_k=\mathbb{E}\left[\boldsymbol{g}_k\right]+\operatorname{Cov}\left(\boldsymbol{g}_k,\boldsymbol{y}_{k\mathrm{p}}\right)\operatorname{Cov}(\boldsymbol{y}_{k\mathrm{p}},\boldsymbol{y}_{k\mathrm{p}})^{-1}\left(\boldsymbol{y}_{k\mathrm{p}}-\mathbb{E}\left[\boldsymbol{y}_{k\mathrm{p}}\right]\right),\tag{11}$$

where $\mathbb{E}\left[\boldsymbol{g}_k\right]=0$, $\operatorname{Cov}\left(\boldsymbol{g}_k,\boldsymbol{y}_{k\mathrm{p}}\right)=\mathbb{E}\left[\sqrt{p_{\mathrm{p}}}\boldsymbol{A}\boldsymbol{g}_k\boldsymbol{g}_k^{\mathrm{H}}\right]=\sqrt{p_{\mathrm{p}}}\boldsymbol{A}\boldsymbol{\Lambda}_k$, $\mathbb{E}\left[\boldsymbol{y}_{k\mathrm{p}}\right]=0$ and $\operatorname{Cov}\left(\boldsymbol{y}_{k\mathrm{p}},\boldsymbol{y}_{k\mathrm{p}}\right)$ can be calculated as

$$\begin{aligned}\operatorname{Cov}\left(\boldsymbol{y}_{k\mathrm{p}},\boldsymbol{y}_{k\mathrm{p}}\right)&=\mathbb{E}\left[p_{\mathrm{p}}\boldsymbol{A}^2\boldsymbol{g}_k\boldsymbol{g}_k^{\mathrm{H}}+\boldsymbol{A}^2\boldsymbol{n}_k\boldsymbol{n}_k^{\mathrm{H}}+\boldsymbol{n}_{k\mathrm{q}}\boldsymbol{n}_{k\mathrm{q}}^{\mathrm{H}}\right]\\&=p_{\mathrm{p}}\boldsymbol{A}^2\boldsymbol{\Lambda}_k+\boldsymbol{A}^2\sigma^2+\boldsymbol{A}\left(\mathbf{I}-\boldsymbol{A}\right)\operatorname{diag}\left(p_{\mathrm{p}}\sum_{j=1}^{K}\boldsymbol{\Lambda}_j+\mathbf{I}\right).\end{aligned}\tag{12}$$

Therefore, the channel estimation is given by

$$\hat{\boldsymbol{g}}_k=\sqrt{p_{\mathrm{p}}}\boldsymbol{A}\boldsymbol{\Lambda}_k\left(p_{\mathrm{p}}\boldsymbol{A}^2\boldsymbol{\Lambda}_k+\sigma^2\boldsymbol{A}^2+\boldsymbol{A}\left(\mathbf{I}-\boldsymbol{A}\right)\operatorname{diag}\left(p_{\mathrm{p}}\sum_{j=1}^{K}\boldsymbol{\Lambda}_j+\mathbf{I}\right)\right)^{-1}\boldsymbol{y}_{k\mathrm{p}}.\tag{13}$$

Furthermore, according to [14], $\hat{\boldsymbol{g}}_k$ is equivalent to

$$\hat{\boldsymbol{g}}_k=\left[\sqrt{\beta_{1,k}}\hat{\boldsymbol{h}}_{1,k}^{\mathrm{T}},\sqrt{\beta_{2,k}}\hat{\boldsymbol{h}}_{2,k}^{\mathrm{T}},\ldots,\sqrt{\beta_{M,k}}\hat{\boldsymbol{h}}_{M,k}^{\mathrm{T}}\right],\tag{14}$$

where $\beta_{m,k}$ is the equivalent large-scale fading between the $m$-th RAU and the $k$-th user and can be expressed as

$$\beta_{m,k}=\frac{\alpha_m^2 p_{\mathrm{p}}\lambda_{m,k}^2}{\alpha_m^2 p_{\mathrm{p}}\lambda_{m,k}+\sigma^2\alpha_m^2+\alpha_m\left(1-\alpha_m\right)p_{\mathrm{p}}\sum_{j=1}^{K}\lambda_{m,j}+\alpha_m\left(1-\alpha_m\right)\sigma^2}. \tag{15}$$

$\hat{\boldsymbol{h}}_{m,k}\sim\mathcal{CN}\left(0,\mathbf{I}_N\right)$ represents the equivalent small-scale fast fading between the $m$-th RAU and the $k$-th user, and $\hat{\boldsymbol{h}}_k=[\hat{\boldsymbol{h}}_{1,k}^{\mathrm{T}},\hat{\boldsymbol{h}}_{2,k}^{\mathrm{T}},\ldots,\hat{\boldsymbol{h}}_{M,k}^{\mathrm{T}}]^{\mathrm{T}}\sim\mathcal{CN}\left(0,\mathbf{I}_{MN}\right)$ is expressed as

$$\hat{\boldsymbol{h}}_k=\left(p_{\mathrm{p}}\boldsymbol{A}^2\boldsymbol{\Lambda}_k+\sigma^2\boldsymbol{A}^2+\boldsymbol{A}\left(\mathbf{I}-\boldsymbol{A}\right)\mathrm{diag}\left(p_{\mathrm{p}}\sum_{j=1}^{K}\boldsymbol{\Lambda}_j+\mathbf{I}\right)\right)^{-1/2}\boldsymbol{y}_k. \tag{16}$$

It can be seen from (15) and (16) that, both the large-scale fading and the small-scale fading are related to the number of quantization bit when the quantization process is considered in channel estimation. By dividing the numerator and the denominator of $\beta_{m,k}$ by $\alpha_m^2$, it is obviously seen that the smaller the number of quantization bit is, the smaller the $\alpha_m$ is and the more serious the channel estimation degradation is.

Since $\hat{\boldsymbol{g}}_k\sim\mathcal{CN}\left(0,\mathrm{diag}\left(\beta_{1,k},\beta_{2,k},\ldots,\beta_{M,k}\right)\otimes\mathbf{I}_N\right)$, due to the orthogonality property of MMSE estimation, $\boldsymbol{g}_k$ can be decomposed into

$$\boldsymbol{g}_k=\hat{\boldsymbol{g}}_k+\tilde{\boldsymbol{g}}_k, \tag{17}$$

where $\tilde{\boldsymbol{g}}_k\sim\mathcal{CN}\left(0,\mathrm{diag}\left(\eta_{1,k},\eta_{2,k},\ldots,\eta_{M,k}\right)\otimes\mathbf{I}_N\right)$ denotes channel estimation error and $\eta_{m,k}\triangleq\lambda_{m,k}-\beta_{m,k}$.

## 3 Spectral efficiency and energy efficiency analysis

In this section, we derive the closed-form expressions of uplink achievable rates with MRC receiver and ZF receiver, and we analyze the system power consumption to obtain the expressions of SE and EE. Based on the closed-form expressions, the SE-EE tradeoff will be analyzed in Section 5.

### 3.1 Spectral efficiency analysis

During the uplink data transmission phase, the signal sent by the $k$-th user is received by the linear receiver and is quantized by ADCs at RAUs which can be expressed as

$$r_k=\boldsymbol{a}_k^{\mathrm{H}}\boldsymbol{y}_{\mathrm{q}}=\sqrt{p_{\mathrm{u}}}\sum_{j=1}^{K}\boldsymbol{a}_k^{\mathrm{H}}\boldsymbol{A}\hat{\boldsymbol{g}}_j x_j+\sqrt{p_{\mathrm{u}}}\sum_{j=1}^{K}\boldsymbol{a}_k^{\mathrm{H}}\boldsymbol{A}\tilde{\boldsymbol{g}}_j x_j+\boldsymbol{a}_k^{\mathrm{H}}\boldsymbol{A}\boldsymbol{n}+\boldsymbol{a}_k^{\mathrm{H}}\boldsymbol{n}_{\mathrm{q}}, \tag{18}$$

where $\boldsymbol{a}_k$ represents the receiver vector, $x_j\sim\mathcal{CN}\left(0,1\right)$ represents the signal transmitted by the $j$-th user. MRC receiver and ZF receiver are considered as

$$\boldsymbol{a}_k=\begin{cases}\hat{\boldsymbol{g}}_k, & \text{for MRC},\\ \boldsymbol{f}_k, & \text{for ZF},\end{cases} \tag{19}$$

where $\boldsymbol{f}_k$ is the $k$-th column of $\hat{\boldsymbol{G}}\left(\hat{\boldsymbol{G}}^{\mathrm{H}}\hat{\boldsymbol{G}}\right)^{-1}$ while $\hat{\boldsymbol{G}}=[\hat{\boldsymbol{g}}_1,\hat{\boldsymbol{g}}_2,\ldots,\hat{\boldsymbol{g}}_K]$. When regarding the inference as irrelevant additive noise [15,16], the uplink achievable rate of the $k$-th user can be given by

$$\begin{aligned}R_k\left(\boldsymbol{b}\right)&=\mathbb{E}\left[\log_2\left(1+\frac{p_{\mathrm{u}}\left|\boldsymbol{a}_k^{\mathrm{H}}\boldsymbol{A}\hat{\boldsymbol{g}}_k\right|^2}{\mathbb{E}[\boldsymbol{a}_k^{\mathrm{H}}(p_{\mathrm{u}}\sum_{j\neq k}\boldsymbol{A}\hat{\boldsymbol{g}}_j\hat{\boldsymbol{g}}_j^{\mathrm{H}}\boldsymbol{A}^{\mathrm{H}}+p_{\mathrm{u}}\sum_j\boldsymbol{A}\tilde{\boldsymbol{g}}_j\tilde{\boldsymbol{g}}_j^{\mathrm{H}}\boldsymbol{A}^{\mathrm{H}}+\boldsymbol{A}^2\sigma^2+\boldsymbol{R}_{\boldsymbol{n}_{\mathrm{q}}})\boldsymbol{a}_k|\hat{\boldsymbol{G}}]}\right)\right]\\&\overset{(a)}{=}\mathbb{E}\left[\log_2\left(1+\frac{p_{\mathrm{u}}\left|\boldsymbol{a}_k^{\mathrm{H}}\boldsymbol{A}\hat{\boldsymbol{g}}_k\right|^2}{\mathbb{E}[\psi_k+\|\boldsymbol{a}_k^{\mathrm{H}}\boldsymbol{A}\|^2]}\right)\right],\end{aligned} \tag{20}$$

where $\boldsymbol{b}=[b_1,b_2,\ldots,b_M]$ denotes quantization bit vector of $M$ RAUs, (a) results from the nature of the conditional expectation and the independence between the estimated channel vector and the estimated channel error vector, and $\psi_k$ can be expressed as

$$\psi_k = p_{\mathrm{u}}\sum_{j\neq k}\boldsymbol{a}_k^{\mathrm{H}}\mathbb{E}\left[\boldsymbol{A}\hat{\boldsymbol{g}}_j\hat{\boldsymbol{g}}_j^{\mathrm{H}}\boldsymbol{A}^{\mathrm{H}}\right]\boldsymbol{a}_k + p_{\mathrm{u}}\sum_{j}\boldsymbol{a}_k^{\mathrm{H}}\mathbb{E}\left[\boldsymbol{A}\tilde{\boldsymbol{g}}_j\tilde{\boldsymbol{g}}_j^{\mathrm{H}}\boldsymbol{A}^{\mathrm{H}}\right]\boldsymbol{a}_k + \boldsymbol{a}_k^{\mathrm{H}}\boldsymbol{R}_{\boldsymbol{n}_{\mathrm{q}}}\boldsymbol{a}_k. \tag{21}$$

In the following, we derive the closed-form expressions of the uplink achievable rates with MRC receiver and ZF receiver, respectively.

**Theorem 1.** With low-precision ADCs, the closed-form expressions of uplink achievable rates can be given by (22) with MRC receiver and by (23) with ZF receiver

$$R_k^{\mathrm{mrc}} = \log_2\left(1+\frac{p_{\mathrm{u}}\sum_{m=1}^{M}\alpha_m^2\beta_{m,k}^2 + p_{\mathrm{u}}N\Gamma_k^2}{\Phi_k+\Theta_k+\Psi_k+\sum_m\alpha_m\beta_{m,k}}\right), \tag{22}$$

where $\Gamma_k = \sum_{m=1}^{M}\alpha_m\beta_{m,k}$, $\Phi_k = p_{\mathrm{u}}\sum_{j\neq k}\sum_m\alpha_m^2\beta_{m,j}\beta_{m,k}$, $\Theta_k = p_{\mathrm{u}}\sum_j\sum_m\alpha_m^2\eta_{m,j}\beta_{m,k}$, $\Psi_k = p_{\mathrm{u}}\sum_m\sum_j t_m\beta_{m,k}\lambda_{m,j}$, $t_m=\alpha_m(1-\alpha_m)$,

$$R_k^{\mathrm{zf}} = \log_2\left(1+\frac{p_{\mathrm{u}}(MN-K+1)\sum_{m=1}^{M}\alpha_m^2\beta_{m,k}}{\Upsilon_k+\Omega_k+\Xi_k+\sum_m\alpha_m}\right), \tag{23}$$

where $\Upsilon_k = p_{\mathrm{u}}\sum_m\sum_{j\neq k}\alpha_m^2\beta_{m,j}$, $\Omega_k = p_{\mathrm{u}}\sum_m\sum_j\alpha_m^2\eta_{m,j}$, $\Xi_k = p_{\mathrm{u}}\sum_m\sum_j t_m\lambda_{m,j}$, $t_m=\alpha_m(1-\alpha_m)$.

**Remark 1.** As seen from (22) and (23), quantization noise affects both the numerator and denominator of (20), which means that the quantization noise affects both useful signals and interference signals. Based on the above theorem, we analyze the progressive performance of the system when quantization bit; the transmission power per user, or the number of antennas per RAU tends to infinity, respectively. The results will be given in Section 5.

### 3.2 Energy efficiency analysis

The power consumption of cell-free massive MIMO systems can be modeled as [3, 17–19]

$$P_{\mathrm{total}}(\boldsymbol{b}) = \sum_{k=1}^{K}P_k + \sum_{m=1}^{M}P_m(b_m) + \sum_{m=1}^{M}P_{\mathrm{bh},m}(\boldsymbol{b}) + P_{\mathrm{CPU}}, \tag{24}$$

where $P_k$ represents the power consumption of the $k$-th user, $P_m(b_m)$ represents the power consumption at the $m$-th RAU, $P_{\mathrm{bh},m}(\boldsymbol{b})$ represents the power consumption of the backhaul link between the $m$-th RAU and the CPU, $P_{\mathrm{CPU}}$ represents the power consumption for baseband signal processing at CPU, $\boldsymbol{b}=[b_1,b_2,\ldots,b_M]$ represents the number of quantization bit vector at $M$ RAUs. Specifically, $P_k$ is expressed as

$$P_k = \frac{p_u}{\xi}N_0 + P_{\mathrm{tc},k}, \tag{25}$$

where $\xi$ is the amplifier efficiency, $N_0$ is the noise power and $P_{\mathrm{tc},k}$ denotes the power consumed by the operation of circuit components of the $k$-th user. Because we only consider the uplink transmission, $P_k$ has no concern with $\boldsymbol{b}$. Moreover, $P_m(b_m)$ is given by

$$P_m(b_m) = N(2c_mP_{\mathrm{AGC},m} + 2P_{\mathrm{ADC},m}(b_m) + P_{\mathrm{res},m}) + P_{\mathrm{LO},m}, \tag{26}$$

where $P_{\mathrm{AGC},m}$, $P_{\mathrm{ADC},m}(b_m)$, $P_{\mathrm{res},m}$ denote the power consumed by AGC, ADC and the residual circuit units per RF link, respectively, and $P_{\mathrm{LO},m}$ represents the power consumption of local oscillator at the $m$-th RAU. In detail, $c_m$ is set as

$$c_m = \begin{cases} 0, & b_m = 1, \\ 1, & b_m > 1, \end{cases} \tag{27}$$

and $P_{\mathrm{ADC},m}(b_m)$ is

$$P_{\mathrm{ADC},m}(b_m) = \mathrm{FOM}_W\cdot f_{\mathrm{s}}\cdot 2^{b_m}, \tag{28}$$

where $\mathrm{FOM}_W$ is the Walden's figure-of-merit [20], and $f_{\mathrm{s}}$ is the Nyquist sampling rate. $P_{\mathrm{bh},m}(\boldsymbol{b})$ can be expressed as

$$P_{\mathrm{bh},m}(\boldsymbol{b}) = P_{0,m} + BP_{\mathrm{bt},m}\sum_{k=1}^{K} R_k(\boldsymbol{b}), \tag{29}$$

where $P_{0,m}$ is the fix power consumption of each backhaul link, $B$ is the bandwidth and $P_{\mathrm{bt},m}$ is the traffic-dependent backhaul link power between the $m$-th RAU and the CPU. Finally, $P_{\mathrm{CPU}}$ can be expressed by

$$P_{\mathrm{CPU}} = MP_{\mathrm{BB}}, \tag{30}$$

where $P_{\mathrm{BB}}$ denotes the power for processing baseband signal for each RAU at CPU.

EE can be modeled as the ratio of the sum of achievable rates to total energy consumption [21, 22] when the unit of energy consumption is watt. The EE can be expressed as

$$\varphi(\boldsymbol{b}) = \frac{B\sum_{k=1}^{K} R_k(\boldsymbol{b})}{P_{\mathrm{total}}(\boldsymbol{b})}. \tag{31}$$

**Remark 2.** As seen from (24) and (31), the quantization bit at RAUs has an influence on both system power consumption and EE. Therefore, we analyze how the quantization bit, the number of antennas per RAU and the transmit power per user influence EE in Section 5.

## 4 The optimization of quantization bit allocation

In this section, we propose feasible quantization bit allocation algorithms to realize the joint optimization of SE and EE with low-precision ADCs in cell-free massive MIMO systems. As shown in (22)–(24), the precision of ADCs determines the SE and power consumption, which in turn affects EE in (31). Hence, the allocation of quantization bit plays an important role in improving system performance. It is proved that compared with the use of fixed high-precision ADCs, the adaptive quantization bit allocation mechanism has the advantages of higher flexibility and lower power consumption by applying variable low-precision ADCs. However, the low-precision ADCs have a bad effect on the SE. Consequently, it is necessary to obtain a good tradeoff between SE and EE through the optimization of the number of quantization bit at RAUs.

### 4.1 Joint optimization problem formulation

The first optimization objective is to maximize the average uplink achievable rate per user.

**Problem 1** (Spectral efficiency maximization)**.**

$$\underset{\boldsymbol{b}}{\text{maximize}} \quad f_1(\boldsymbol{b}) = \sum_j R_j^v(\boldsymbol{b})/K, \tag{32}$$

where $v$ represents MRC or ZF receiver. In cell-free massive MIMO systems, the impact of small-scale fading is minimal and users pay more attention to the average QoS. It is reasonable to simply use the closed-form expressions of the achievable rates only related to the large scale for optimization.

The second optimization objective is to maximize the EE.

**Problem 2** (Energy efficiency maximization)**.**

$$\underset{\boldsymbol{b}}{\text{maximize}} \quad f_2(\boldsymbol{b}) = \varphi(\boldsymbol{b}). \tag{33}$$

It is noteworthy that the distributions of RAUs are considered in the optimization objectives which is the key of feasible quantization bit allocation algorithm. Besides, the total number of quantization bit is limited to make sure the optimization results are within a reasonable range, and the minimum uplink achievable rate per user is limited to ensure the QoS in practical situation. We assume all users send signals at full power and there are perfect ADCs at users. Thus, we obtain a joint optimization problem which can be formulated as the following.

**Problem 3** (Joint optimization problem)**.**

$$\begin{aligned} \underset{\boldsymbol{b}}{\text{maximize}} \quad & \boldsymbol{f} = [f_1(\boldsymbol{b}), f_2(\boldsymbol{b})]^{\mathrm{T}} \\ \text{s.t.} \quad & \mathrm{C1}: R_k^{\mathrm{ul}} \geqslant R_k^{\mathrm{ul,min}}, \qquad \forall k = 1, 2, \ldots, K, \\ & \mathrm{C2}: N \sum_m b_m \leqslant b_{\mathrm{total}}, \quad \forall m = 1, 2, \ldots, M, \end{aligned} \tag{34}$$

where $b_{\mathrm{total}}$ is the total number of quantization bit at all RAUs. The great tradeoff between SE and EE simultaneously can be achieved by solving (34).

### 4.2 Solutions to SE and EE tradeoff

The existence of the non-convexity and discrete optimization variables of each objective makes it challenging to obtain the solutions due to the increasing complexity by traditional optimization ways. Consequently, we propose one solution based on DQN and the one solution based on NSGA-II to solve the joint optimization problem.

#### 4.2.1 *Solution based on DQN*

In the optimization problem, the model describes the relationship between the optimal quantization bit allocation and the location distributions of RAUs and users are unknown. Q-learning mechanism has advantages of discovering how to choose actions to maximize the reward and achieve the goal [23], so it is suitable for the optimization problem. In the proposed algorithm, the state $s_t$ in Q-learning mechanism is defined as

$$s_t \triangleq \boldsymbol{b}_t, \tag{35}$$

where $\boldsymbol{b}_t$ represents the quantization bit vector in step $t$. The action $a_t$ is defined as

$$a_t \triangleq \tilde{\boldsymbol{b}}_t, \tag{36}$$

where $\tilde{\boldsymbol{b}}_t$ represents the change of quantization bit in step $t$ and only one bit can be changed per step. The reward $r_t$ is defined as

$$r_t \triangleq f_1(\boldsymbol{b}) + f_2(\boldsymbol{b}) / 10^5 - \tilde{r}, \tag{37}$$

where $f_1(\boldsymbol{b})$ in (32) denotes average SE, $f_2(\boldsymbol{b})$ in (33) denotes EE and $\tilde{r}$ is a constant related to the sum of SE and EE. To ensure the joint optimization of SE and EE, we divide EE by $10^5$ so that SE and EE are on the same order of magnitude.

Considering the choice of action in step $t$, we take the state-action $Q$ values as the basis and the epsilon greedy scheme is applied. In step $t$, the state-action $Q$ value of each possible action in state $s_t$ is estimated. The action with the greatest $Q$ value will be selected if the random probability is less than the fixed probability $\varepsilon$. Otherwise, the action will be chosen randomly.

Nevertheless, the state space and action space are so big that it is difficult to find a state-action $Q$ value table. Thus, it is necessary to introduce the neural network to obtain state-action $Q$ values. The input of the neural network is state $s_t$ and the output of the neural network is the $Q$ values of all actions in state $s_t$. The parameters of the neural network are optimized by performing a gradient descent step on the squared error loss which can be expressed as

$$y_t = \left( r_t + \gamma \max_{a' \in A} Q(s', a') - Q(s_t, a_t) \right)^2, \tag{38}$$

where $r_t$ is the reward of action $a_t$ in the step $t$, $\gamma$ denotes the discount parameter, $Q(s_t, a_t)$ denotes the $Q$ value of the selected action $a_t$ in the state $s_t$, and $\max_{a' \in A} Q(s', a')$ represents the maximal state-action $Q$ value of the next state $s'$, and $A$ is the set of actions. The computational complexity of solution based on DQN mainly results from the matrix multiplication in forward propagation and backward propagation of deep neural network. Therefore, the computational complexity of the algorithm based on DQN is $O(2(Mn_1 + 2Mn_{L-1} + \sum_{l=2}^{L-1} n_{l-1} n_l) s_t)$, where $M = 20$ denotes the number of RAUs and the number of nodes of input layer, $2M$ denotes the total number of actions and the number of nodes of output layer, $L = 2$ denotes the number of network layers, $n_l$ denotes the number of nodes of $l$-th

layer, $s = 32$ represents the size of mini-batch and $t = 80000$ represents the number of iterations [24] in the optimization problem.

The quantization bit allocation algorithm based on DQN is summarized in Algorithm 1.

**Algorithm 1** Quantization bit allocation algorithm based on DQN

Initialize the state $s_0$ and the parameters of neural network;
**while** $t < t_{\max}$ **do**
  Select action $a_t$ based on epsilon greedy scheme and state-action $Q$ values;
  Obtain the next sate $s'$;
  Calculate the reward $r_t$ of action $a_t$ in step $t$;
  Save $s_t$, $a_t$, $r_t$ and $s'$ for the neural network optimization;
  $t = t + 1$;
**end while**
Output the state $s_{\max}$ with the greatest reward.

#### 4.2.2 *Solution based on NSGA-II*

Although the DQN bit allocation algorithm can optimize SE and EE jointly by maximizing the sum of SE and EE, we cannot take insight into the SE-EE Pareto boundary. The multi-objective evolutionary algorithm NSGA-II is proved efficient to solve our proposed optimization problem [25]. NSGA-II can solve all optimization objectives at the same time to find the Pareto-optimal SE-EE tradeoff front which allows us to choose the number of quantization bit flexibly according to the demand. The computational complexity of NSGA-II to obtain all the Pareto-optimal solutions in our problem is $O(2S^2)$ where $S$ denotes the population size which corresponds to the number of Pareto-optimal solutions.

To apply NSGA-II, first of all, we initialize the algorithm parameters related to NSGA-II: the maximum iterations $G_{\max}$, the size of population $p$, the distribution index for crossover etac and for mutation etam, and so on. Secondly, $p$ quantization bit vectors $\boldsymbol{b}$ are randomly generated under the constrain C2 which is denoted as population $P^{(0)}$. The population $P^{(0)}$ is ranked based on non-dominating sorting and crowding distance. Thirdly, select a parent population by tournament selection according to the currently ranked population and generate offspring population by selection, mutation, and crossing. Fourthly, combine the offspring population and the old population to sort a new population $P^{(\text{generation})}$ including $p$ solutions based on the rank results. Then repeat the second step to the fourth step until the generation reaches $G_{\max}$. Finally, output the optimal population $P^{G_{\max}}$ with $\boldsymbol{f}$ in (34).

The steps of the quantization bit allocation algorithm based on NSGA-II are shown in Algorithm 2.

**Algorithm 2** Quantization bit allocation algorithm based on NSGA-II

Initialize system parameters: the maximum iterations $G_{\max}$, the size of population $p$, generation = 1;
Generate the population $P^{(0)}$ randomly and rank each individual based on non-dominating sorting and crowding distance;
**while** generation $\leqslant G_{\max}$ **do**
  Select an excellent parent population to generate offspring population by selection, mutation, and crossing;
  Rank the offspring population and the old population to generate a new population $P^{(\text{generation})}$;
  generation = generation + 1;
**end while**
Output the optimal population $P^{G_{\max}}$ with $\boldsymbol{f}$ in (34).

## 5 Simulation results

In this section, the accuracy of the closed-form expressions is verified by simulations and the impact of low-precision ADCs on system SE and EE is analyzed. Besides, we present the simulation results to evaluate the performance of our proposed quantization bit allocation algorithms based on SE-EE joint optimization.

This paper assumes a circular area with a radius $R = 1000$ m. There are $K = 5$ uplink users and they are all uniformly distributed in the area with a minimum access distance $r_0 = 30$ m to RAUs. According to [16], the path loss exponent between the $k$-th user and the $m$-th RAU is modeled as $\lambda_{m,k} = d_{m,k}^{-l}$, where $d_{m,k}$ denotes the distance between the $k$-th user and the $m$-th RAU, $l$ is the path loss exponent which is set as 3.7. Besides, the length of uplink pilot sequence is $\tau = K$ and the coherence time in symbols is $T = 196$. All the power consumption parameters are given in Table 2 according to [3, 19].

**Table 2** Power consumption parameters

| Parameter | Value |
|---|---|
| $p_{\mathrm{u}}$ | 0.02 W |
| $N_0$ | $290 \times \kappa \times B \times \mathrm{NF}$ |
| $\kappa$ | $1.381 \times 10^{-23}$ J/K |
| $B$ | 1 MHz |
| NF | 9 dB |
| $\xi$ | 0.4 |
| $P_{tc,k}$ | 100 mW |
| $P_{\mathrm{AGC},m}$, $P_{\mathrm{res},m}$, $P_{\mathrm{LO},m}$ | 2 mW, 20 mW, 22.5 mW |
| $\mathrm{FOM}_W$ | 15 fJ/conversion-step |
| $P_{0,m}$, $P_{\mathrm{bt},m}$ | 200 mW, 0.25 W/(Gbits/s) |
| $P_{\mathrm{BB}}$ | 200 mW |

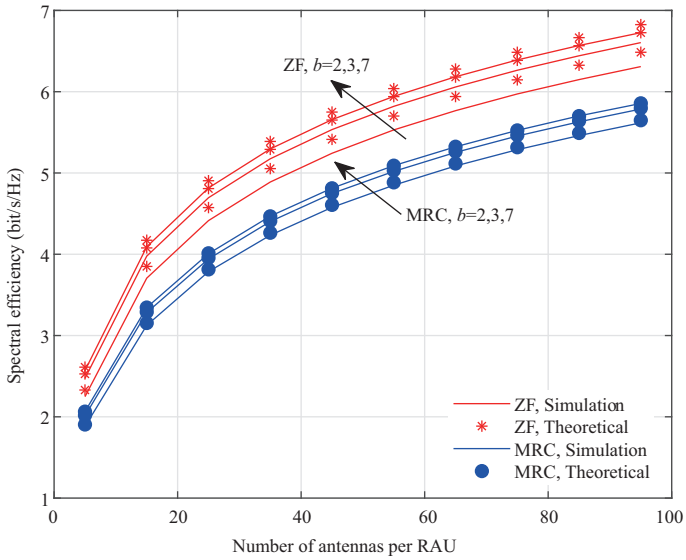


**Figure 1** (Color online) Uplink average SE against the number of antennas per RAU when $M = 6$.

Firstly, we verify the accuracy of the closed-form expressions of uplink achievable rate given by Theorem 1. Figure 1 shows the relationship between the average uplink SE and the number of antennas at each RAU when the number of quantization bit $b$ varies. Regardless of the number of quantization bit per RAU, the closed-form expressions of achievable rate are consistent with the simulation results, which proves the correctness of Theorem 1. However, the smaller the number of quantization bit is, the greater the gap between the simulated results and theoretical results is which results from the bigger quantization noise when estimating channel. And ZF receiver is more easily affected by low-precision ADCs. Furthermore, when the number of quantization bit is fixed, as the number of antennas per RAU increases, the uplink SE increases and the gap between MRC and ZF receiver gets larger due to the ability of ZF receiver to resist interference. Considering the fixed number of antennas per RAU, as the number of quantization bit increases, the uplink SE increases rapidly when $b \leqslant 3$. However, the increase of $b$ hardly further improves the uplink SE when $b \geqslant 3$. It leads to that low-precision ADCs can be used in massive MIMO systems, and adding antennas of each RAU can compensate for the performance impairment caused by low-precision ADCs to a certain extent.

Next, we study the power-scaling law of SE. Considering that the number of quantization bit is fixed, each user's transmit power is $p_{\mathrm{u}} = E_{\mathrm{u}}/(MN)$ with fixed $E_{\mathrm{u}} = 2$ W when $N$ changes. Figure 2 illustrates the uplink average SE under different numbers of quantization bit against the number of antennas per RAU with MRC receiver and ZF receiver. It can be seen that as the number of antennas $N$ increases, the uplink SE increases, but the growth rate gradually slows down. When $N$ is fixed, the SE increases and performance gain decreases as $b$ increases. When $b < 4$, the SE grows when $b$ grows. When $b \geqslant 4$, the SE almost keeps the same no matter how $b$ increases. The SE approaches the limit rate when $b \to \infty$, $N \to \infty$. When $N$ is small, compared with the decrease in SE caused by the decrease in uplink

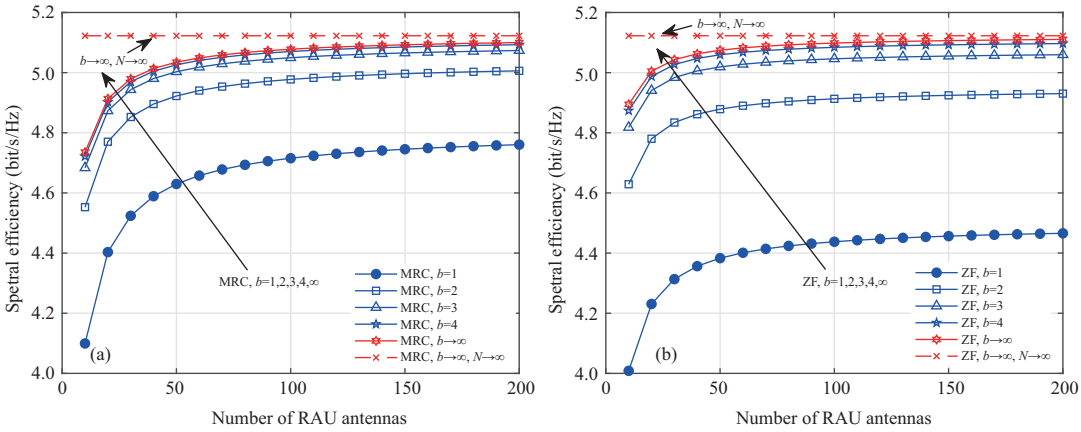


**Figure 2** (Color online) Uplink average SE against the number of antennas and the number of quantization bit per RAU when $p_{\mathrm{u}} = E_{\mathrm{u}}/(MN)$, $M = 25$. (a) MRC receiver; (b) ZF receiver.

transmission power, the increase in SE caused by the increase in the number of antennas plays a major role. Therefore, the increase in SE is fast. As $N$ increases, the influence of the decrease in the uplink transmission power and the increase in the number of antennas gradually reaches a balance, so the SE increases slowly and gradually tends to a certain value. When we focus on the difference between MRC receiver and ZF receiver, it seems that ZF receiver is more sensitive to the damage brought by the low-precision ADC. When $b$ increases, the SE increases more rapidly with ZF receiver especially when $b < 4$. Though the limit rates of MRC receiver and ZF receiver are almost at the same, the ZF receiver exceeds MRC receiver under the same condition and ZF receiver can reach the limit faster.

Then, we make an intensive study of the relationship between SE and EE. We discuss the relationship from the perspective of the number of quantization bit, number of antennas per RAU and transmit power per user. Figure 3 illustrates the SE changes against EE when the number of quantization bit and the number of antennas change. In the figure, different lines correspond to different number of quantization bit ($b = [1, 2, 3, 6, 8]$), and different points on each line correspond to different number of antennas per RAU ($N = [1 : 3 : 80]$). As the number of antennas per RAU increases, the SE gradually increases, but the EE firstly increases and then decreases. When comparing different curves, as the number of quantization bit increases, the SE increases more and more slowly, but the EE firstly increases and then decreases. This is because power consumption and SE increase with the increase of the number of antennas and the number of quantization bit. When the number of antennas or the number of quantization bit is small, the increase in SE plays a major role. However, as the number of antennas or the number of quantization bit increases, the increase in power consumption gradually plays a major role. There is a little difference with the trend of the curves when $b \geqslant 6$ which can be explained by the rapid growth of the power consumption and the slow growth of the SE when the number of quantization bit $b > 5$ according to Theorem 1 and (24). Drawing a comparison between MRC receiver and ZF receiver, ZF receiver has better performance than MRC receiver on both SE and EE in general. However, when the number of quantization bit per RAU $b = 1$ and the number of antennas per RAU $N < 5$, the performance of MRC receiver is better. It suggests that the performance of ZF receiver benefits a little from multi-antenna structure but gets a lot loss from 1 bit ADCs when the number of antennas per RAU is small.

Figure 4 shows the relationship between SE and EE when the number of quantization bit and the transmit power per user change. In the figure, different lines correspond to different number of quantization bit ($b = [1, 2, 3, 4, 5, 6, 7]$) per RAU, and different points on each line correspond to different transmit power at each user ($p_{\mathrm{u}} = [0.001, 0.002, 0.01, 0.05, 0.1, 0.3, 0.8, 1.2, 1.8, 2.5, 3.5]$). As the transmit power per user increases, the SE firstly increases rapidly and then increases very slowly; the EE firstly increases and then decreases rapidly. It proves that the SE will reach the limit when transmit power increases to a high value so the EE will drop rapidly. In other words, increasing transmit power per user can only compensate for the damage caused by low-precision ADC and improve system performance to a certain extent. Besides, when the transmit power is low, the performance of ZF receiver is seriously affected whatever the number of quantization bit is. But as the increase of the transmit power, the performance improves faster with ZF receiver than with MRC receiver.

Based on the above analysis, it is more appropriate to set the number of quantization bit as 2–4 bit

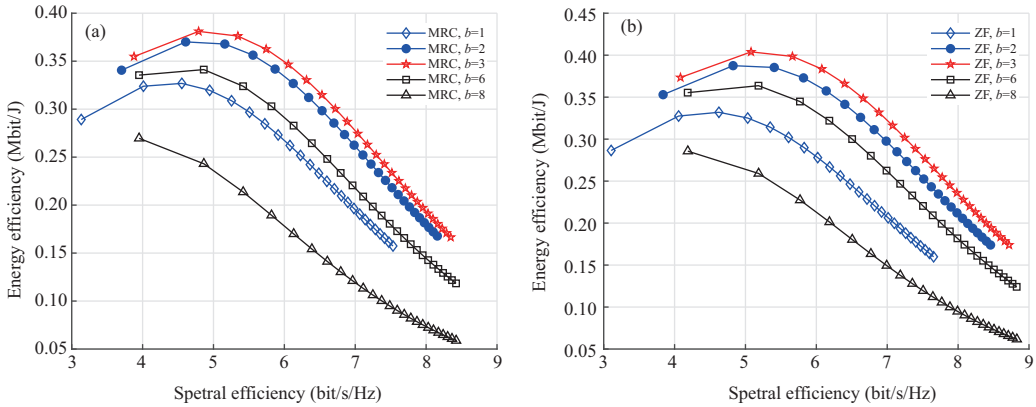


**Figure 3** (Color online) Tradeoff between SE and EE against the number of quantization bit and the number of antennas per RAU, $M = 25$. (a) MRC receiver; (b) ZF receiver.

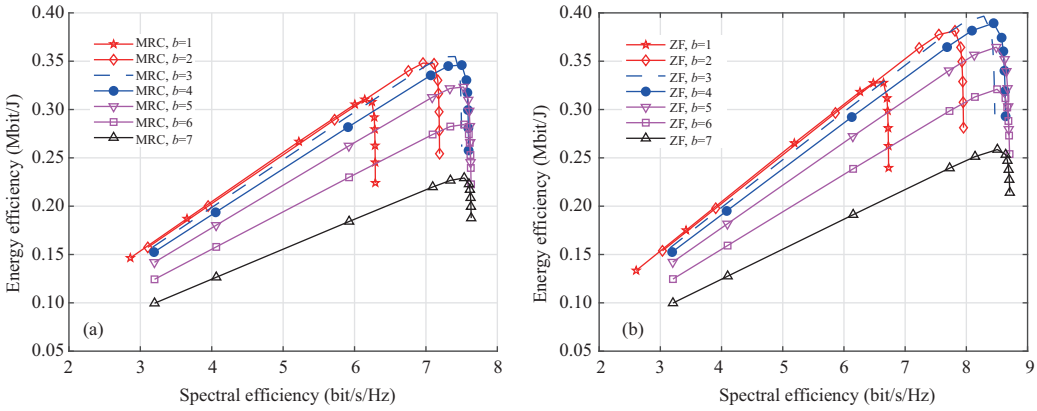


**Figure 4** (Color online) Tradeoff between SE and EE against the number of quantization bit ($b = [1, 2, 3, 4, 5, 6, 7]$) and the transmit power per user, $M = 25$. (a) MRC receiver; (b) ZF receiver.

despite of the receiver when the precision of all ADCs at one RAU is the same and RAUs are distributed uniformly. But it should be noted that the optimal number of quantization bit of ADCs depends on the system parameters and system configuration. Moreover, we cannot improve SE and EE at the same time infinitely and need to weigh the two. It will be discussed in the following.

We assume that ADCs on different RAUs can choose different number of quantization bit, but the ADCs on the same RAU have the same number of quantization bit. Figure 5 shows the Pareto boundary of SE-EE joint optimization with MRC and ZF receiver obtained by solving (34) using NSGA-II when RAUs are uniformly distributed. The number of RAU is $M = 20$ and the total number of quantization bit is $160N$. The required minimum signal-to-interference-plus-noise ratio (SINR) of each user is set to 5 dB. Each point represents a bit allocation solution, and the corresponding SE and EE are shown in the horizontal and vertical coordinate, respectively. The optimal allocation of quantization bit tends to be the equal quantization bit allocation when RAUs are uniformly distributed on a circle that surrounds the uniformly distributed users. The results revealed by the figure are in accordance with the former analysis when receiver or the number of antennas changes. The ZF receiver outperforms MRC receiver both in SE and EE. Similar to Figure 3, when the number of antennas per RAU increases from 4 to 15, the SE increases and the EE first increases slightly and then decreases. The EE decreases monotonically with the increase of SE, so the EE and SE cannot be maximized simultaneously. But we find more feasible solutions to the allocation of the quantization bit of ADCs.

When it comes to the non-uniform distributions of RAUs, as shown in Figure 6, we compare the performance of equal quantization bit allocation algorithm and our proposed algorithms when ZF receiver is applied. The figure illustrates that our proposed algorithms exceed the equal quantization bit allocation algorithm both in SE and EE. To be specific, when the quantization bit per RAU is 4 in equal quantization bit allocation algorithm, the performance of bit vector $\boldsymbol{b} = [4, 5, 1, 1, 1, 6, 5, 1, 1, 4, 1, 6, 1, 1, 3, 4, 5, 1, 4, 4]$ is much better. It seems that the fewer total number of quantization bit achieves better performance

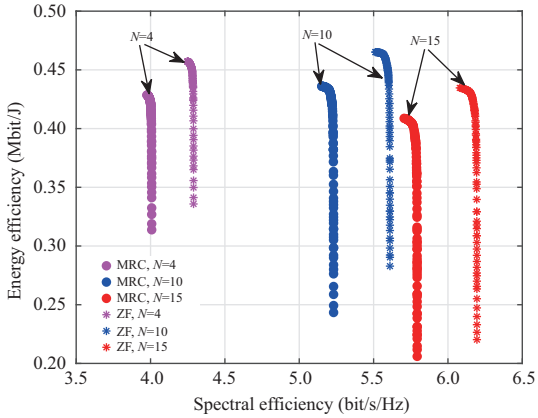


**Figure 5** (Color online) Pareto boundary of SE and EE joint optimization.

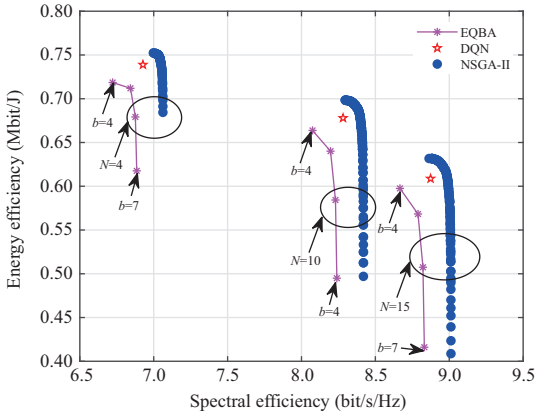


**Figure 6** (Color online) Comparison between equal quantization bit allocation algorithm (EQBA) and our proposed algorithms.

**Table 3** Allocation of quantization bit based on DQN

| $N$ | RAU distribution | $\boldsymbol{b}$ | SE (bit/s/Hz) | EE (Mbit/J) |
|---|---|---|---|---|
| 4 | Uniform | [4, 2, 3, 4, 4, 3, 3, 4, 4, 3, 3, 4, 4, 3, 4, 4, 4, 3, 4, 2] | 4.2109 | 0.4538 |
| 10 | Uniform | [4, 5, 3, 4, 4, 3, 3, 4, 4, 3, 3, 4, 5, 3, 4, 2, 4, 3, 4, 3] | 5.5392 | 0.4591 |
| 15 | Uniform | [4, 3, 3, 5, 4, 3, 3, 4, 3, 3, 3, 4, 4, 3, 4, 2, 3, 4, 2, 3] | 6.0213 | 0.4296 |
| 4 | Non-uniform | [5, 4, 2, 1, 1, 6, 4, 1, 1, 3, 1, 7, 1, 1, 5, 3, 3, 1, 2, 3] | 6.9271 | 0.7389 |
| 10 | Non-uniform | [5, 4, 1, 1, 1, 6, 4, 1, 1, 3, 1, 7, 1, 1, 5, 3, 3, 1, 3, 3] | 8.3014 | 0.6794 |
| 15 | Non-uniform | [5, 5, 2, 1, 1, 6, 5, 1, 1, 3, 1, 6, 1, 1, 5, 3, 3, 1, 2, 3] | 8.8942 | 0.6142 |

**Table 4** Pareto-optimal allocation of quantization bit

| $N$ | RAU distribution | $\boldsymbol{b}$ | SE (bit/s/Hz) | EE (Mbit/J) |
|---|---|---|---|---|
| 4 | Uniform | [4, 4, 3, 4, 4, 3, 3, 4, 4, 3, 3, 4, 4, 3, 4, 4, 4, 3, 4, 4] | 4.2489 | 0.4571 |
| 4 | Uniform | [5, 5, 4, 5, 5, 5, 4, 5, 5, 5, 4, 5, 5, 4, 5, 5, 5, 4, 5, 5] | 4.2789 | 0.4488 |
| 4 | Non-uniform | [4, 5, 1, 1, 1, 6, 5, 1, 1, 4, 1, 6, 1, 1, 3, 4, 5, 1, 4, 4] | 7.0278 | 0.7505 |
| 4 | Non-uniform | [5, 6, 1, 1, 1, 6, 6, 1, 1, 5, 1, 6, 1, 1, 3, 4, 5, 1, 4, 5] | 7.0380 | 0.7499 |

because the distributions of RAUs are taken into account. Generally speaking, the RAUs which far away from users should be allocated fewer quantization bit while the RAUs near the user center can be equipped with higher-precision ADCs, especially in the cell-free massive MIMO scenario. It should be noted that the NSGA-II algorithm provides more feasible and effective solutions than equal quantization bit allocation algorithm when the number of quantization bit $b \leqslant 5$ . In addition, the solution obtained by DQN is close to the Pareto-boundary obtained by NSGA-II when $M$ is large and the iteration is limited. The DQN algorithm runs faster than the NSGA-II algorithm but the NSGA-II algorithm uncovers the Pareto-optimal front.

When ZF receiver is applied, the optimal bit allocation schemes obtained by DQN algorithm in a given iteration are listed in Table 3. As seen from Table 3, the optimal solutions tend to be the same despite the number of antennas per RAU. Similarly, the Pareto-optimal solutions with NSGA-II are almost the same when the number of antennas per RAU varies. So the quantization bit allocation solutions with NSGA-II are partly shown in Table 4 when $N = 4$. In Table 4, as the number of quantization bit decreases, the SE goes down slightly and the EE goes up. It suggests that the reasonable allocation of quantization bit can reduce the total number of quantization bit while maintaining good performance. Moreover, we can provide more feasible solutions to various SE and EE requirements. As Tables 3 and 4 shown, the allocation of quantization bit tends to be equal when RAUs are uniformly distributed. However, when RAUs are random non-uniformly distributed, the allocation of quantization bit depends on distributions of RAUs. In other words, the proposed quantization bit allocation algorithms adapt to the changes of RAU positions which proves the effectiveness of the proposed algorithms.

## 6 Conclusion

In this paper, we derived the closed-form expressions of the uplink achievable rates applying MRC receiver and ZF receiver based on the estimated CSI in cell-free massive MIMO systems with low-precision ADCs. The simulation results showed that the SE hardly increases when the number of quantization bit $b > 5$ and ZF receiver are more sensitive to 1-bit ADCs and 2-bit ADCs. The SE will reach the upper limit fast as the number of antennas per RAU increases if the user power is limited. Next, the system EE was modeled which is related to the number of quantization bit at RAUs. Then we analyzed the trade-off between SE and EE. It is presented that the EE firstly increases and then decreases as the number of antennas per RAU, the transmit power or the number of quantization bit increase. The optimal number of quantization bit of the system is 2–4 bit when RAUs are uniformly distributed. Furthermore, we proposed two optimization algorithms for the allocation of quantization bit based on DQN and NSGA-II to optimize SE and EE jointly. The DQN quantization bit allocation algorithm solves the problem faster and finds the bit vector which maximizes the sum of SE and EE, while the NSGA-II quantization bit allocation algorithm provides all the Pareto-optimal solutions. The simulation results proved the proposed algorithms which are adaptive to the positions of RAUs are superior to the equal quantization bit allocation algorithm.

**Acknowledgements** This work was supported in part by National Key Research and Development Program (Grant No. 2020YFB1806600), National Natural Science Foundation of China (Grant Nos. 61971127, 61871465, 61871122), and Fundamental Research Funds for the Central Universities.

**References**

1 Ngo H Q, Ashikhmin A, Yang H, et al. Cell-free massive MIMO versus small cells. IEEE Trans Wireless Commun, 2017, 16: 1834–1850

2 Hu X L, Zhong C J, Chen X M, et al. Cell-free massive MIMO systems with low resolution ADCs. IEEE Trans Commun, 2019, 67: 6844–6857

3 Zhang Y, Zhou M, Qiao X, et al. On the performance of cell-free massive MIMO with low-resolution ADCs. IEEE Access, 2019, 7: 117968–117977

4 Bai X B, Zhou M, Qiao X, et al. Uplink performance analysis of cell-free MIMO with low-resolution ADCs and ZF receiver. In: Procceedings of the 22nd International Conference on Advanced Communication Technology (ICACT), Phoenix Park, 2020. 125–129

5 Zhang Y, Cheng Y L, Zhou M, et al. Analysis of uplink cell-free massive MIMO system with mixed-ADC/DAC receiver. IEEE Syst J, 2020. doi: 10.1109/JSYST.2020.2999521

6 Verenzuela D, Björnson E, Matthaiou M. Hardware design and optimal ADC resolution for uplink massive MIMO systems. In: Procceedings of 2016 IEEE Sensor Array and Multichannel Signal Processing Workshop (SAM), Rio de Janerio, 2016. 1–5

7 Liu T T, Tong J, Guo Q H, et al. Energy efficiency of massive MIMO systems with low-resolution ADCs and successive interference cancellation. IEEE Trans Wireless Commun, 2019, 18: 3987–4002

8 Pirzadeh H, Swindlehurst A L. Spectral efficiency under energy constraint for mixed-ADC MRC massive MIMO. IEEE Signal Process Lett, 2017, 24: 1847–1851

9 Roth K, Nossek J A. Achievable rate and energy efficiency of hybrid and digital beamforming receivers with low resolution ADC. IEEE J Sel Areas Commun, 2017, 35: 2056–2068

10 Bai Q, Nossek J A. Energy efficiency maximization for 5G multi-antenna receivers. Trans Emerging Tel Tech, 2015, 26: 3–14

11 Ding Q F, Jing Y D. Spectral-energy efficiency tradeoff in mixed-ADC massive MIMO uplink with imperfect CSI. Chin J Electron, 2019, 28: 618–624

12 Pitarokoilis A, Mohammed S K, Larsson E G. Uplink performance of time-reversal MRC in massive MIMO systems subject to phase noise. IEEE Trans Wireless Commun, 2015, 14: 711–723

13 Bjornson E, Matthaiou M, Debbah M. Massive MIMO with non-ideal arbitrary arrays: hardware scaling laws and circuit-aware design. IEEE Trans Wireless Commun, 2015, 14: 4353–4368

14 Li J M, Wang D M, Zhu P C, et al. Uplink spectral efficiency analysis of distributed massive MIMO with channel impairments. IEEE Access, 2017, 5: 5020–5030

15 Ngo H Q, Larsson E G, Marzetta T L. Energy and spectral efficiency of very large multiuser MIMO systems. IEEE Trans Commun, 2013, 61: 1436–1449

16 Li J M, Wang D M, Zhu P C, et al. Spectral efficiency analysis of single-cell multi-user large-scale distributed antenna system. IET Commun, 2014, 8: 2213–2221

17 Zhang J, Dai L, He Z, et al. Mixed-ADC/DAC multipair massive MIMO relaying systems: performance analysis and power optimization. IEEE Trans Commun, 2019, 67: 140–153

18 Ngo H Q, Tran L N, Duong T Q, et al. On the total energy efficiency of cell-free massive MIMO. IEEE Trans Green Commun Netw, 2018, 2: 25–39

19 Zhang J, Dai L L, He Z Y, et al. Performance analysis of mixed-ADC massive MIMO systems over rician fading channels. IEEE J Sel Areas Commun, 2017, 35: 1327–1338

20 Walden R H. Analog-to-digital converter survey and analysis. IEEE J Sel Areas Commun, 1999, 17: 539–550

21 Zuo J, Zhang J, Yuen C, et al. Energy-efficient downlink transmission for multicell massive DAS with pilot contamination. IEEE Trans Veh Technol, 2017, 66: 1209–1221

22 Bjornson E, Sanguinetti L, Hoydis J, et al. Optimal design of energy-efficient multi-user MIMO systems: is massive MIMO the answer? IEEE Trans Wireless Commun, 2015, 14: 3059–3075

23 Le T D, Le A T, Nguyen D T. Model-based Q-learning for humanoid robots. In: Proceedings of the 18th International Conference on Advanced Robotics (ICAR), Hong Kong, 2017. 608–613

24 Xu J, Zhu P C, Li J, et al. Deep learning-based pilot design for multi-user distributed massive MIMO systems. IEEE Wireless Commun Lett, 2019, 8: 1016–1019

25 Qatab W S A, Alias M Y, Ku I. Optimization of multi-objective resource allocation problem in cognitive radio LTE/LTE-A femtocell networks using NSGA-II. In: Proceedings of IEEE 4th International Symposium on Telecommunication Technologies (ISTT), Selangor, 2018. 1–6